Autonomic healing of thermoplastic elastomer composed of triblock copolymer

Ritsuko Watanabe,[1] Takumi Sako,[1] Suphat Korkiatithaweechai,[1] Masayuki Yamaguchi[1]*

[1]School of Materials Science, Japan Advanced Institute of Science and Technology, 1-1 Asahidai, Nomi, Ishikawa 923-1292, Japan

*Corresponding author
E-mail: m_yama@jaist.ac.jp
Tel: +81-761-51-1621; Fax: +81-761-51-1149

Abstract

In this paper, we demonstrated that commercially available triblock copolymers such as polystyrene-*b*-polybutadiene-*b*-polystyrene (SBS) and polystyrene-*b*-polyisoprene-*b*-polystyrene (SIS), used as thermoplastic elastomers, exhibit autonomic self-healing behavior at room temperature without any chemical reaction even after cutting into two separate pieces. The healing efficiency is improved by immediate recombination after cutting, and is attributed to the destruction of the microstructure, i.e., polystyrene domains, leading to marked molecular mobility. Furthermore, quenched samples with obscure phase-separation exhibit good healing behavior. Finally, SBS has better healing efficiency than SIS because the solubility parameter of polybutadiene is closer to that of polystyrene than that of polyisoprene; to some extent, the solubility parameter is responsible for enhanced molecular motion owing to the mutual dissolution of both components.

Keywords: thermoplastic elastomer; triblock copolymer; self-healing; viscoelastic properties

INTRODUCTION

It is well known that triblock copolymers have microstructures, such as spheres, cylinders, gyroids, and lamellae, which are basically determined by the compatibility, volume fraction, and molecular weight of the components [1–6]. Ambient temperature, flow field, and the addition of another component such as a plasticizer also affect the structure [4–13]. Although detailed academic studies on the microdomain structure of triblock copolymers have been carried out, the use of such copolymers in industrial applications such as thermoplastic elastomer, adhesive, and impact modifier for thermoplastic resins have reemphasized the importance of a basic understanding of their structure [5, 14]. Of the triblock copolymers, polystyrene-*b*-polybutadiene-*b*-polystyrene (SBS), polystyrene-*b*-polyisoprene-*b*-polystyrene (SIS), and polystyrene-*b*-(ethylene-*co*-1-butene)-*b*-polystyrene (SEBS) are the most readily available materials in industry. When the Shell Oil Company began to commercially manufacture SBS in 1964, one of their objectives was to provide an alternative for vulcanized rubber, because SBS acts as a thermoplastic elastomer [5].

In this paper, we demonstrate that commercially available SBS and SIS can exhibit self-healing behavior without any manual intervention. Although they have been used

as a substitute for vulcanized rubber for a long time, to the best of our knowledge their self-healing behavior has not been reported.

There have been several approaches to the material design of self-healing polymers [15-19]. In this study, the interdiffusion of polymer chains through the boundary of the cut surface is used to repair triblock copolymers such as SBS and SIS. Such a mechanism was originally proposed by Wool [15]. He found that rubber autohesion can be attributed to the interdiffusion of molecular chains, and explained this phenomenon using the tube model [20]. Self-healing is detected even for plastics when the ambient temperature is above the glass transition temperature (T_g); this is known as crack healing or thermal healing. However, because a material can flow macroscopically at temperature above the T_g, the phenomenon has not been exploited for the design of self-healing polymers. Yamaguchi et al. proposed a new design for a self-healing polymer in which the interdiffusion of dangling chains in a weak gel would be responsible for healing [21-23]. Above the T_g, dangling chains show marked diffusion through the boundary, leading to self-healing behavior. Moreover, the material would never flow macroscopically because of the permanent network. Yamaguchi's team also found that poly(ethylene-*co*-vinyl acetate), which has a low degree of crystallinity, exhibits self-healing behavior [24]. Because crystallites act as crosslink points, the

material shows a similar mechanical behavior to a weak gel above the T_g. This material has the disadvantage of poor heat resistance because it has a low melting point and a sticky surface due to low crystallinity. In this study, we demonstrate the self-healing property of SBS and SIS. Because commercially available SBS and SIS do not have sticky surfaces, this interesting property could be beneficial to certain applications.

MATERIALS AND METHODS

Materials and sample preparation

We used commercially available SBS with a styrene content of 24 wt.% (TR2827, JSR, Japan), kindly provided by the JSR Corporation, and SIS with a styrene content of 18 wt.% (SEPTON2004, Kuraray, Japan), kindly provided by Kuraray Co., Ltd. The number- and weight-average molecular weights (M_n and M_w, respectively), evaluated by size exclusion chromatography (HLC-8020, Tosoh, Japan) with TSK-GEL GMHXL using chloroform as a solvent and as a polystyrene standard, were $M_n = 9.5 \times 10^4$ and $M_w = 1.1 \times 10^5$ for SBS, and $M_n = 8.7 \times 10^4$ and $M_w = 9.0 \times 10^4$ for SIS.

The sample was compressed into a flat sheet using a compression-molding machine as follows. After pre-heating in the machine at 160°C for 5 min, the sample was compressed under 20 MPa for 2 min. The sheet was subsequently cooled to 25°C for 3

min using another compression-molding machine. Another compressed sheet was prepared at 200°C and cooled to 5°C to investigate the effect of the processing conditions on the microstructure and healing properties. In this paper, the samples heated at 160°C are referred to as “slow-cooling”, and the samples heated at 200°C are called “rapid-cooling”. Once the sheets had been prepared they were immediately used for the measurements.

Measurements

We measured the oscillatory shear modulus as a function of angular frequency using a strain-controlled rheometer with a parallel-plate geometry (MR-500, UBM, Japan) at 160°C and 200°C. The circular plates (25 mm in diameter) were separated by a distance of approximately 0.9 mm.

The small-angle X-ray scattering pattern was measured using an X-ray diffractometer (SmartLab, Rigaku, Japan). The thickness of the specimen was 3 mm. The measurements were performed using CuKα radiation operating at 40 kV and 30 mA at a scanning speed of 0.50 degree·min^{-1}.

The temperature dependence of the oscillatory tensile modulus of the samples was evaluated with a rectangular specimen (5 mm × 20 mm × 1 mm) using a dynamic

mechanical analyzer (E4000-DVE, UBM, Japan) in the temperature range from −120 to 150°C. The frequency and heating rate used were 10 Hz and 2°C·min^{-1}, respectively. The self-healing property of each sample was evaluated using a uniaxial tensile machine (LSC-50/300, Tokyo Testing Machine, Japan) at 25°C. The crosshead speed was 10 mm·min^{-1} and the initial gauge length was 10 mm. The sample preparation method is shown in Fig. 1.

[Fig. 1]

After the rectangular virgin samples (10 mm × 30 mm × 3 mm) had been prepared by cutting the compressed sheet, they were further cut into two pieces using a razor blade at room temperature. The cut surfaces of the pieces were immediately jointed together by manual operation. A slight pressure, that was removed after recombination, was applied initially to promote perfect attachment of the surfaces, i.e., wetting. According to Wool, the level of an applied pressure has no/little impact on the healing, i.e., mutual diffusion, as long as surfaces are jointed perfectly [15]. The recombined pieces were stored in a temperature- and humidity-controlled chamber (IG420, Yamato, Japan) at 25°C and 50% relative humidity for various times, i.e., healing periods. Moreover, some of the cut pieces were kept in the temperature- and

131 humidity-controlled chamber before the recombination. All tensile tests were performed
132 at least 10 times and the average value was calculated.
133 The surface free energies of the compressed sheet and cut surface were evaluated by
134 measurements of the contact angle (Drop Master DM-301, Kyowa, Japan). The surface
135 free energy was calculated according to the acid-base theory. To determine the surface
136 free energy components and parameters of a solid, the contact angles of three liquids,
137 such as water, ethylene glycol, and diiodomethane, were measured.
138

139 **Results and discussion**

140 **Effect of processing condition on morphology**

141 Figure 2 shows the angular frequency dependence of the shear storage modulus G' and
142 the loss modulus G'' measured at 160°C and 200°C of SBS. The sample prepared by the
143 slow-cooling was employed. A plateau modulus in the low frequency region, i.e., the
144 network structure, is clearly discernable at 160°C, suggesting that polystyrene (PS)
145 microdomains still existed at that temperature even beyond the T_g of PS. In contrast,
146 both moduli decreased rapidly with decreasing angular frequency at 200°C, indicating
147 that mutual dissolution of PS and polybutadiene (PB) blocks occurred, at least to some

148 degree. The results demonstrate that the system shows thermorheological complexity, as
149 reported [25]. The order–disorder transition occurred between 160 and 200°C.

150 [Fig. 2]

151 The microstructure of the sample in the solid state was evaluated by small-angle X-ray
152 scattering, as shown in Fig. 3. The slow-cooling sample produced a sharp peak, whereas
153 the rapid-cooling sample produced a small peak. The long periods were calculated to be
154 25.6 nm for the slow-cooling sample and 27.2 nm for the rapid-cooling sample. The
155 results suggest that the slow-cooling sample had a well-developed phase-separated
156 structure and the rapid-cooling sample exhibited the rheological properties of the molten
157 state.

158 [Fig. 3]

159 The temperature dependence of the dynamic tensile moduli is shown in Fig. 4. As seen
160 in the figure, double peaks were detected in the E'' and tan δ curves; one is located at
161 approximately −90°C, which can be attributed to the glass transition temperature (T_g) of
162 the PB block, whereas the other is at approximately 90°C, i.e., the T_g of the PS block.
163 Furthermore, the slow-cooling sample shows high-level E' in the rubbery region due to
164 well-developed phase separation. In contrast, there is no obvious peak in the tan δ curve
165 ascribed to the T_g of PS for the rapid-cooling sample. The results indicate that PS

domains are not distinctly formed by rapid cooling because phase separation cannot occur during the cooling process.

[Fig. 4]

Self-healing behavior

Figure 5 shows the stress–strain curves with the photographs of the recombined samples jointed immediately after cutting. The samples were prepared by the slow-cooling. The numerals in the figure represent the healing periods at 25°C in the temperature- and humidity-controlled chamber. The given stresses and strains are the engineering values. It should be noted that the sample with a prolonged healing period had a large strain at break, revealing that SBS exhibited self-healing behavior even at room temperature without any chemical reaction. This result indicates mutual diffusion through the jointed boundary. The phenomenon is interesting because such compressed samples do not have sticky surfaces and therefore never exhibit autohesion. In contrast, the cut surface showed autohesion, i.e., healing. Furthermore, the stress–strain curves for the repaired samples were the same as that of the original compressed sample without cutting, although the strain at break was smaller.

[Fig.5]

Figure 6 shows the stress–strain curves for the samples recombined after leaving the cut surface for 1 week at 25°C. As shown in the figure, the samples showed poor healing, although the strain at break increased slightly with the length of the healing period. This result suggests that the characteristics of the cut surface change with duration of exposure to the atmosphere.

[Fig.6]

We measured the increase in surface tension of the cut surface to evaluate the compositional change after cutting, and found that the surface tension of the cut surface was approximately 32.0 $mJ \cdot m^{-2}$, which is between that of polystyrene (34.3 $mJ \cdot m^{-2}$) and polybutadiene (23.5 $mJ \cdot m^{-2}$) [26]. Furthermore, the value did not change with time, suggesting that the composition of the segments remained constant. Favorable healing behavior was detected in samples recombined immediately after cutting, and many free molecules whose chain ends were not trapped in the PS domains appeared at the cut surface, presumably owing to the extremely large deformation at/near the cutting area. After leaving the cut surface for a while, chain mobility is eventually reduced by the reorganization of the microstructure, i.e., well-developed PS domains on the surface, which leads to poor healing.

The microstructure prior to cutting also affects healing efficiency. As shown in Fig. 7, the rapid-cooling sample exhibited better healing behavior than the slow-cooling sample. The mutual dissolution of both segments in the rapid-cooling sample was responsible for the pronounced molecular mobility.

[Fig.7]

To gain a better understanding of the self-healing behavior of the triblock copolymer, we performed the same experiments using the SIS samples prepared by rapid cooling, i.e., heating to 160°C and cooling to 5°C. Figure 8 shows the dynamic mechanical properties of the SIS samples obtained by the slow-cooling (open symbols) and the rapid cooling (closed symbols). Furthermore, the SBS sample with the rapid cooling was shown by the lines for comparison. The glass-to-rubber transition of PS was clearly detected for SIS, indicating that SIS had well-developed phase-separation compared with SBS (rapid-cooling) obtained under the same cooling conditions. Considering that the PS content in SIS is lower than in SBS, this can be explained by the difference in PS compatibility between PB and polyisoprene (PI). Because the solubility parameter of PI is 16.7 $mJ \cdot m^{-2}$ [26], its compatibility with PS is poor compared with PB.

[Fig.8]

The stress–strain curves of the recombined samples, i.e., the healed samples, are shown in Fig. 9. Both SBS and SIS samples were prepared by the rapid-cooling. It was found that healing efficiency is not as good in the SIS sample as in the SBS samples irrespective of the annealing period. This is as expected because the well-developed PS domains trap the PS segments in SIS and reduce molecular motion, which is responsible for healing.

[Fig. 9]

Conclusion

We investigated the microstructure and self-healing behavior of two commercially available thermoplastic elastomer: polystyrene-*b*-polybutadiene-*b*-polystyrene (SBS) and polystyrene-*b*-polyisoprene-*b*-polystyrene (SIS). First, we found that the triblock copolymers exhibited self-healing behavior at room temperature, whereas the compressed sample pieces did not show autohesion without sticky surfaces. The healing behavior was pronounced in the surfaces of the separate pieces immediately after cutting, although the surface tension of the cut surfaces did not change with time after cutting. Moreover, the sample with well-developed phase-separation showed poor healing behavior. These experimental results indicate that the destruction of the

236 microstructure leads to free molecules in the PS domains, which are responsible for
237 healing. After the reconstruction of the microstructure, therefore, the cut surface loses
238 its healing ability.

239

240 **ACKNOWLEDGEMENTS**

241 This work was promoted by COI program “Construction of next-generation
242 infrastructure system using innovative materials” – Realization of safe and secure
243 society that can coexist with the Earth for centuries – Supported by Japan Science and
244 Technology Agency (JST).

245

246 **References**

247 1. Leibler L (1980) Theory of microphase separation in block copolymers.
248 Macromolecules 13(6):1602-1617
249 2. Khandpur AK, Tomes S, Bates FS (1995) Polyisoprene-polystyrene diblock
250 copolymer phase diagram near the order-disorder transition. Macromolecules 28
251 (26):8796-8806
252 3. Bates FS, Fredrickson GH (1990) Block copolymer thermodynamics: Theory and
253 experiment. Annu Rev Phys Chem 41:525-557

4. Hamley IW (1998) The physics of block copolymers. Oxford University Press, New York
5. Drobny JG (2014) Handbook of thermoplastic elastomers 2nd Ed. Elsevier, Amsterdam
6. Matsushita Y (2015) Block copolymers. In Encyclopedia of polymeric nanomaterials, Kobayashi S, Müllen K Eds. pp. 233-236
7. Kotaka T, Watanabe H (1982) Superstructure and rheology of block copolymer solutions. J Soc Rheol Jpn 10(1):24-38
8. Albalak RJ, Thomas EL (1993) Microphase separation of block copolymer solutions in a flow field. J Polym Sci Polym Phys 31(1):37-46
9. Takahashi Y, Noda M, Ochiai N, Noda I (1996) Shear-rate dependence of first normal stress difference of poly(isoprene-b-styrene) in solution near the order-disorder transition temperature. Polymer 37(26):5943-5945
10. Daniel C, Hamley IW, Mortensen K (2000) Effect of planar extension on the structure and mechanical properties of polystyrene–poly(ethylene-co-butylene)-polystyrene triblock copolymers. Polymer 41(26):9239-9247

11. Hanley KJ, Lodge TP, Huang CI (2000) Phase behavior of a block copolymer in solvents of varying selectivity. Macromolecules 33(16):5918-5931
12. Airey GD (2004) Styrene butadiene styrene polymer modification of road bitumens. J Mater Sci 39(3):951-959
13. Costa P, Silva J, Sencadas V, Simoes R, Viana JC, Lanceros-Mendez S (2013) J Mater Sci 48(3):1172-1179
14. Satas D (1989) Handbook of pressure-sensitive-adhesive technology 2nd ed. Van Nostrand Reinhold, New York
15. Wool RP (1994) Polymer interfaces: Structure and strength. Hanser Gardener, Cincinnati
16. Brown EN, White SR, Sottos NR (2004) Microcapsule induced toughening in a self-healing polymer composite. J Mater Sci 39(5):1703-1710
17. Zhang MQ, Rong MZ (2011) Self-healing polymers and polymer composites. Wiley, Hoboken
18. Herbst F, Döhler D, Michael P, Binder WH (2013) Self-healing polymers via supramolecular forces. Macromol Rapid Commun 34(3):203-220
19. Hu L, Cheng X, Zhang A (2015) A facile method to prepare UV light-triggered self-healing polyphosphazenes. J Mater Sci 50(5):2239-2246.

289 20. Doi M, Edwards SF (1989) The theory of polymer dynamics. Oxford University
290 Press, New York
291 21. Yamaguchi M, Ono S, Terano M (2007) Self-repairing property of polymer network
292 with dangling chains. Mater Lett 61:1396-1399
293 22. Yamaguchi M, Ono S, Okamoto K (2009) Interdiffusion of dangling chains in weak
294 gel and its application to self-repairing material. Mater Sci Eng B 162:189-194
295 23. Yamaguchi M, Maeda R, Kobayashi R, Wada T, Ono S, Nobukawa S (2012)
296 Autonomic healing and welding by interdiffusion of dangling chains in weak gel.
297 Polym Intern 61(1):9-16
298 24. Osato R, Sako T, Seemork J, Arayachukiat S, Nobukawa S, Yamaguchi M (2016)
299 Self-healing properties of poly(ethylene-*co*-vinyl acetate). Colloid Polym Sci
300 294:537-543
301 25. Bates FS (1984) Block copolymers near the microphase separation transition. 2.
302 Linear dynamic mechanical properties. Macromolecules 17(12): 2607-2613
303 26. Brandrup J, Immergut EH, Grulke EA (1998) Polymer handbook Vol. 2. Wiley,
304 New York
305

Figure Captions

Figure 1 Schematic illustration of the sample preparation methods for the self-healing test. All procedures were carried out at 25°C. The dimensions of the initial sample shape before cutting were 10 mm width, 30 mm length, and 3 mm thickness. The samples were cut into two pieces with a razor blade at room temperature. The cut pieces were attached together with a slight pressure immediately after cutting or after leaving the pieces for a week. The recombined samples were then kept in the temperature-humidity controlled chamber at 25 °C for various waiting times (10 min - 72 hr).

Figure 2 Angular frequency dependence of (closed circles) shear storage modulus *G'* and (open circles) loss modulus *G"* at 160°C and 200°C for SBS.

Figure 3 Small-angle X-ray scattering patterns for SBS; (open symbols) slow-cooling and (closed symbols) rapid-cooling.

Figure 4 Temperature dependence of (circles) tensile storage modulus *E'* and (diamonds) loss tangent *tan* δ for SBS; (open symbols) slow-cooling and (closed symbols) rapid-cooling.

Figure 5 Stress-strain curves of the healed samples recombined immediately after cutting for SBS. The samples were obtained by the slow-cooling. The

numerals represent the annealing periods after recombination of the cut pieces. In the figure, photographs at the tensile testing are shown; (blue frame) strain at 0.19 of the sample annealed for 10 min. and (red frame) strain at 0.8 of the sample annealed for 72 hr.

Figure 6 Stress-strain curves of samples with waiting for 1 week after cutting for SBS. The numerals represent the annealing periods after the recombination of the cut pieces.

Figure 7 Strain at break evaluated by tensile tests; (left) the separated pieces were recombined immediately after cutting and (right) the separated pieces were kept at room temperature for 1 week before the recombination. The annealing periods at room temperature after the recombination were 10 min and 72 hr.

Figure 8 Temperature dependence of (circles and solid line) tensile storage modulus *E'* and (diamonds and dotted line) loss tangent *tan δ*; (lines) SBS, rapid-cooling, (open symbols) SIS, slow-cooling, and (closed symbols) SIS, rapid-cooling.

Figure 9 Stress-strain curves of the healed samples recombined immediately after cutting; (open symbols) SIS and (closed symbols) SBS, obtained by the

rapid-cooling. The annealing periods at room temperature after the recombination were (dotted lines) 10 min and (solid lines) 72 hr.

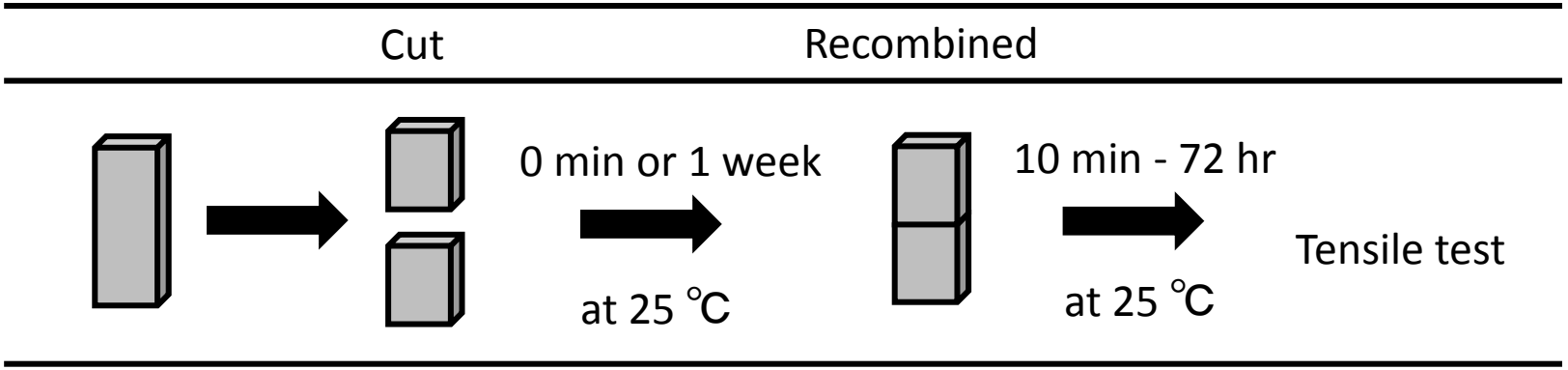

Watanabe et al., Figure 1

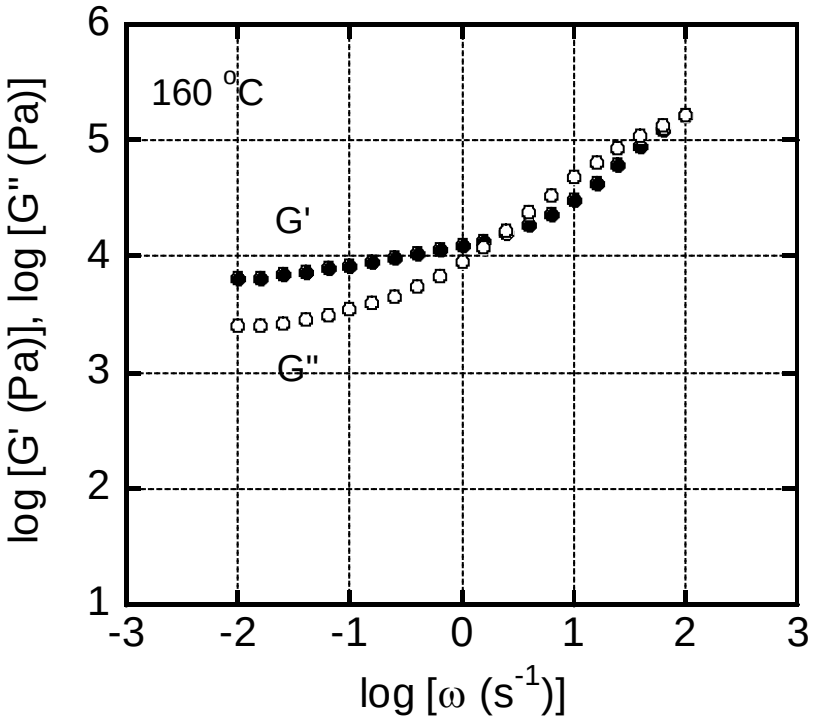

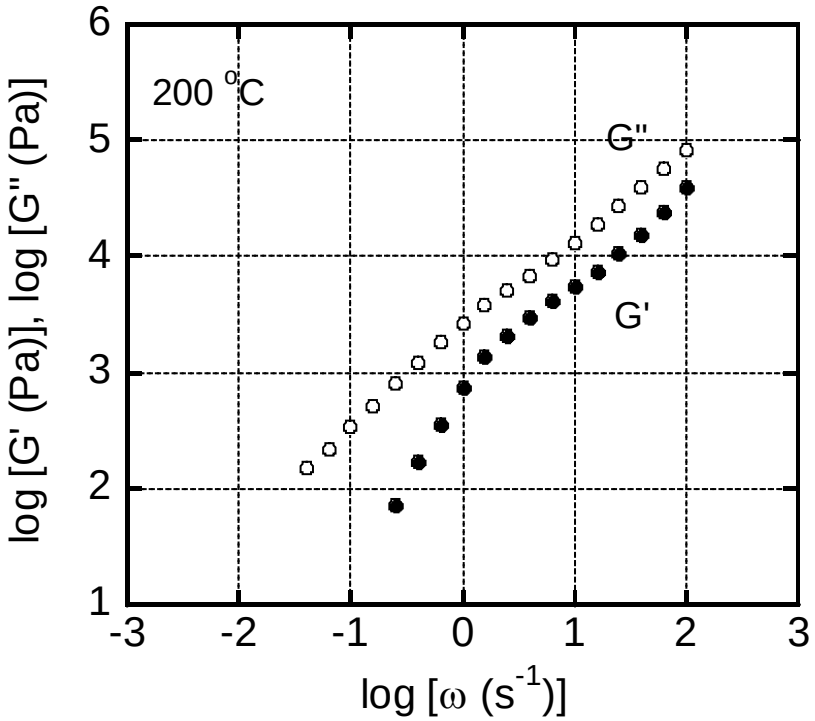

Watanabe et al., Figure 2

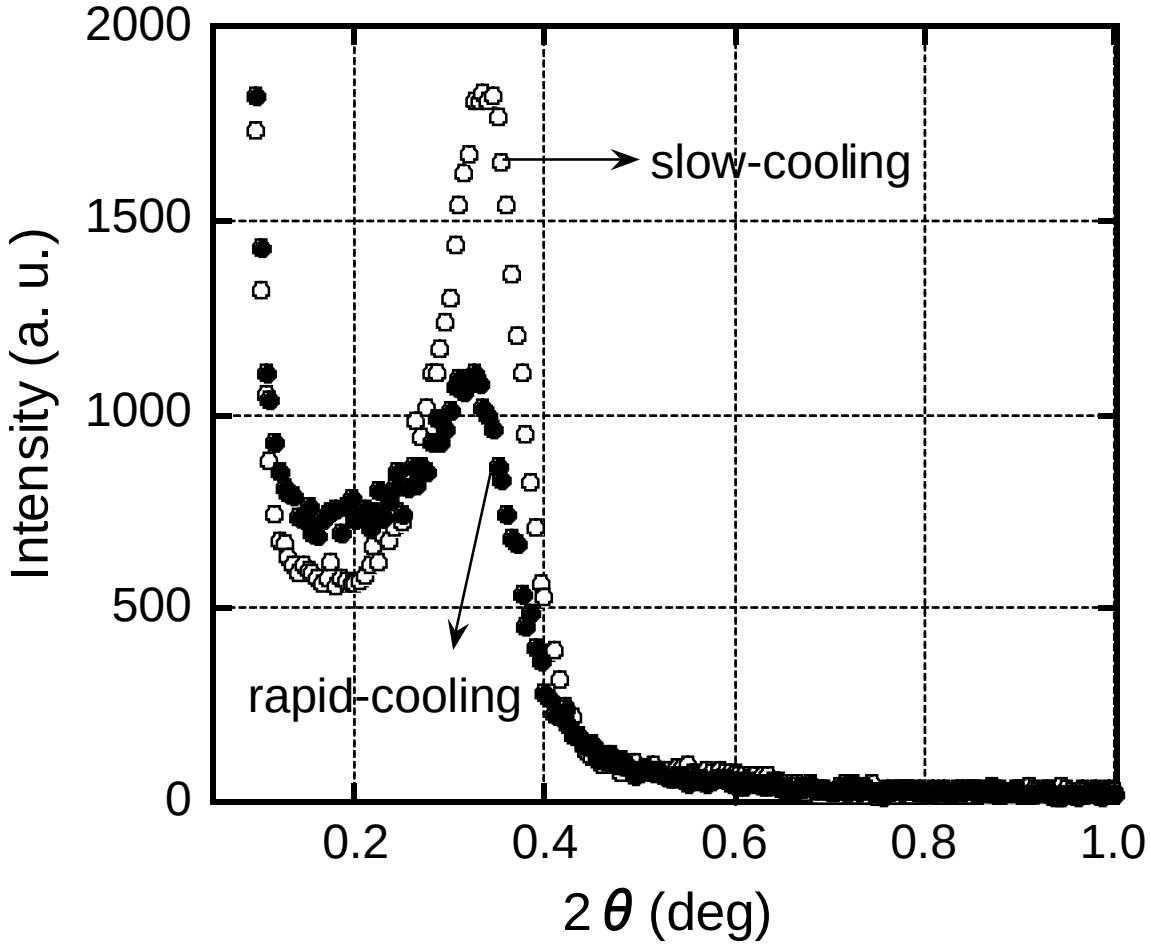

Watanabe et al., Figure 3

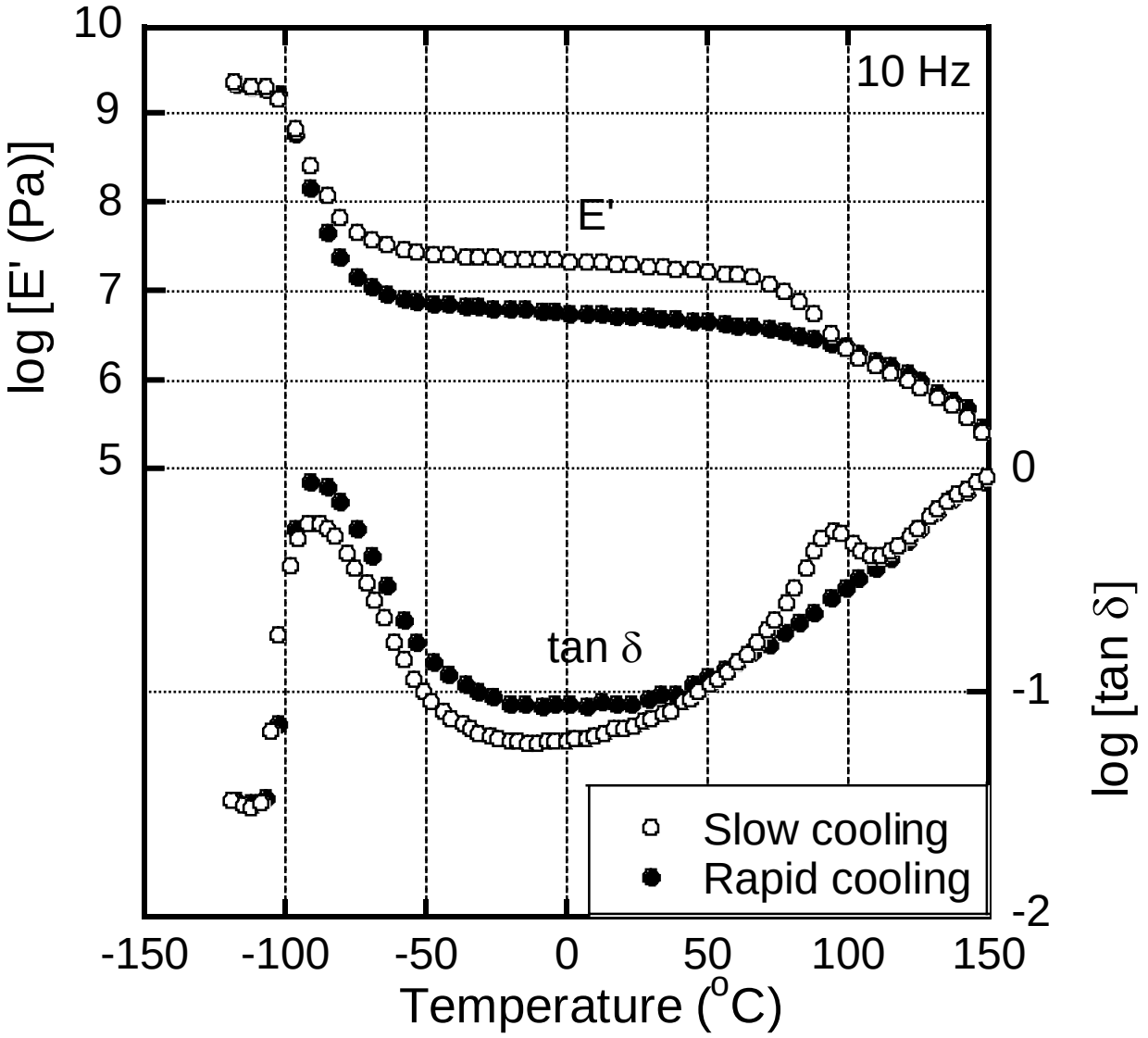

Watanabe et al., Figure 4

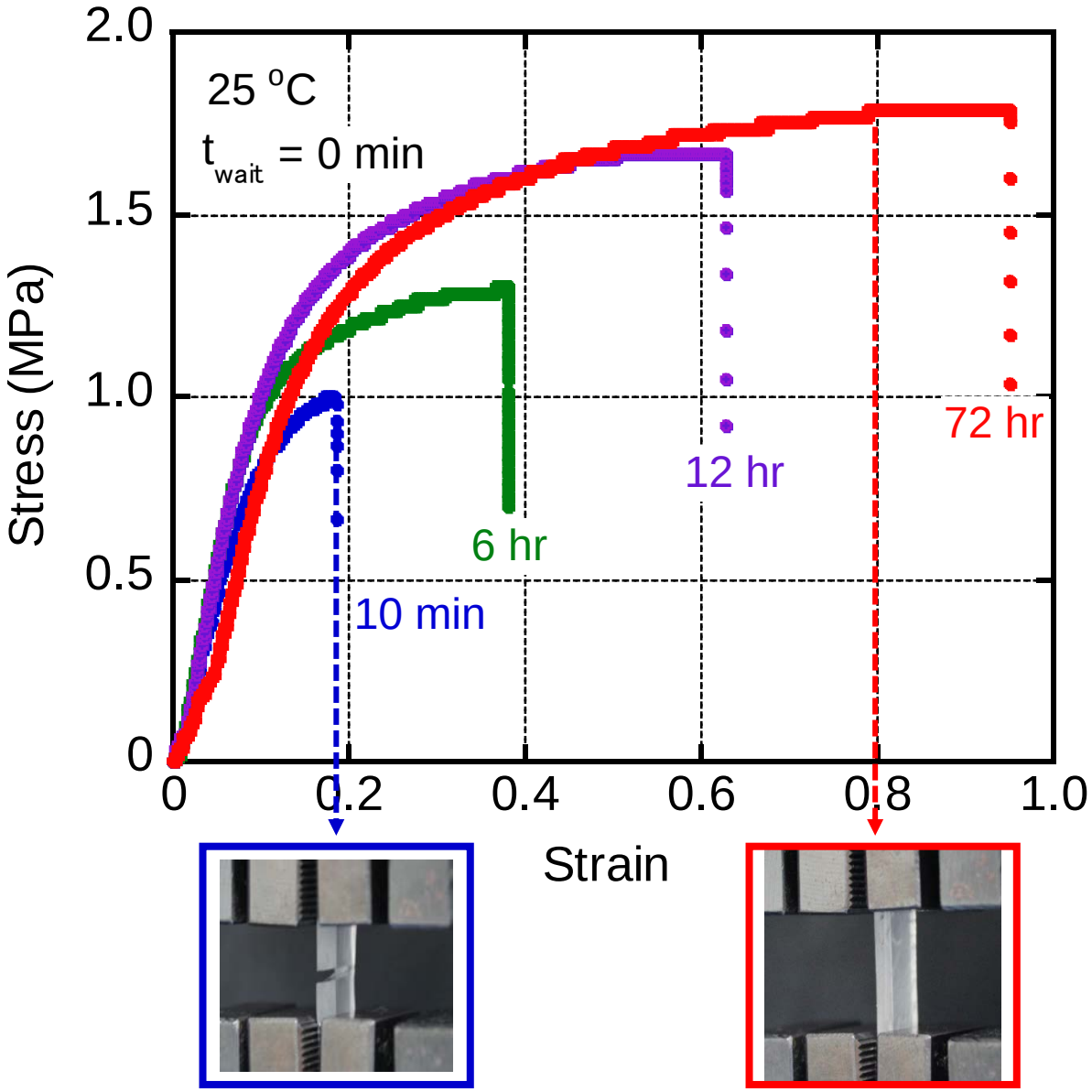

Watanabe et al., Figure 5

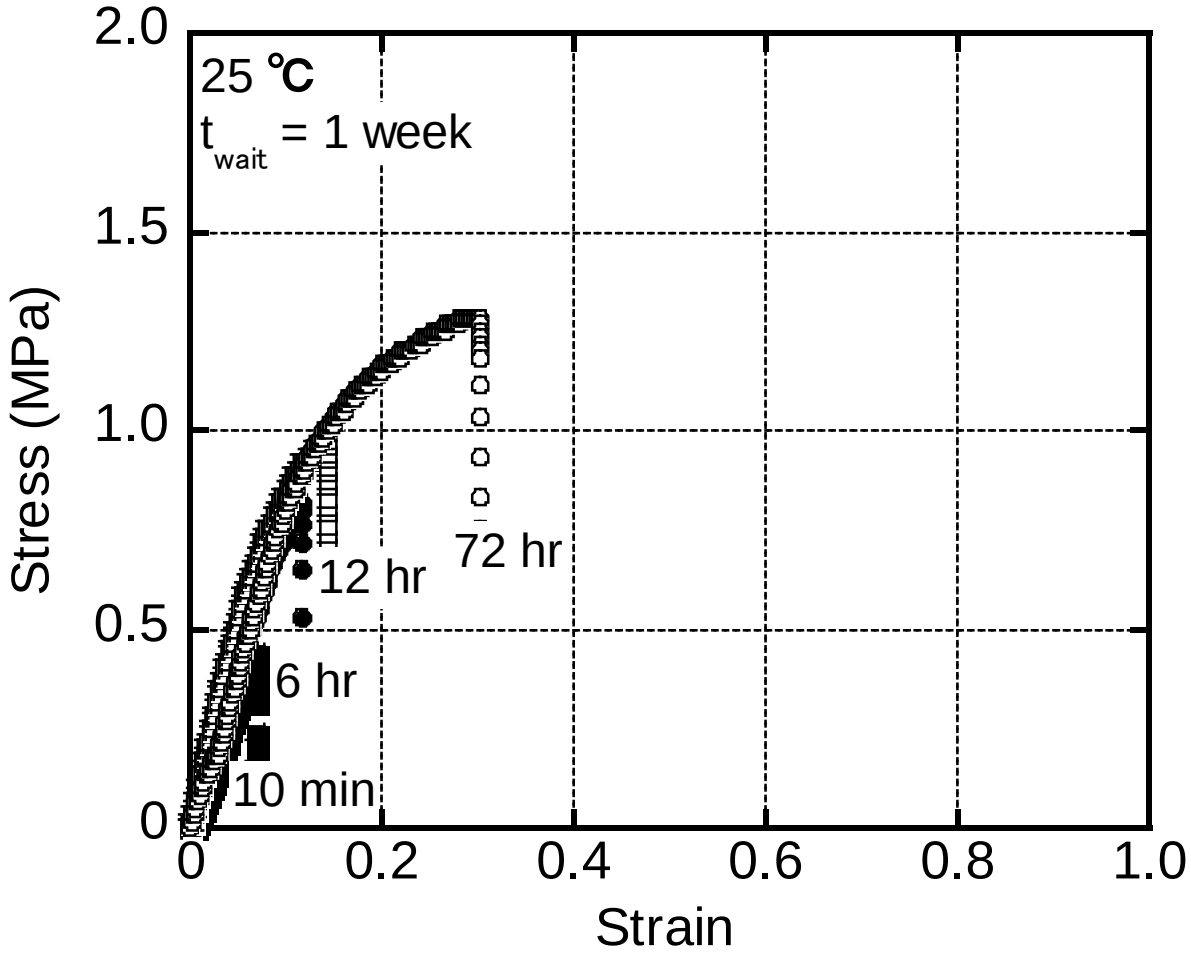

Watanabe et al., Figure 6

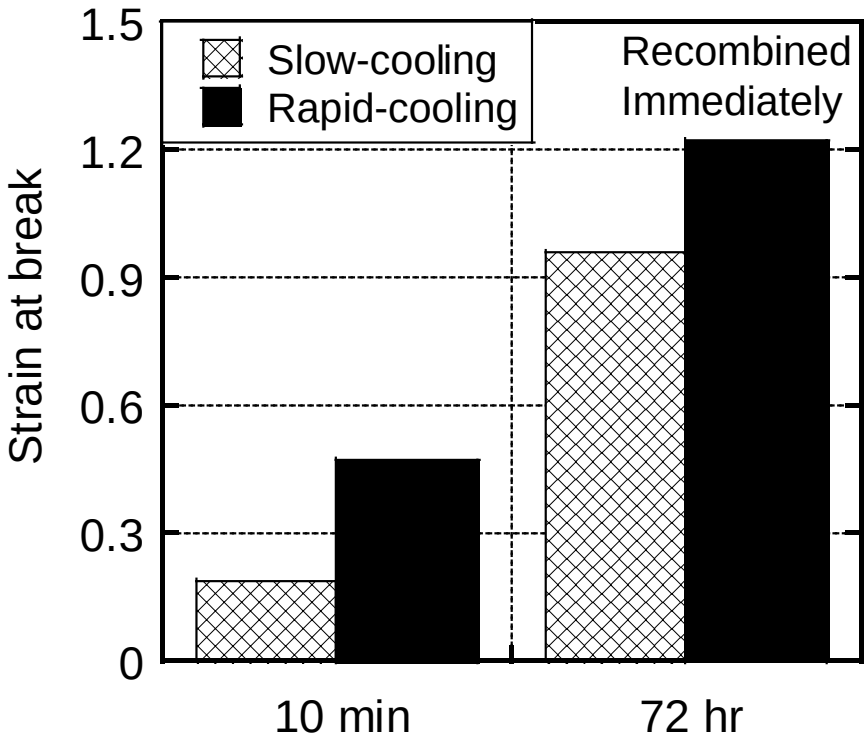

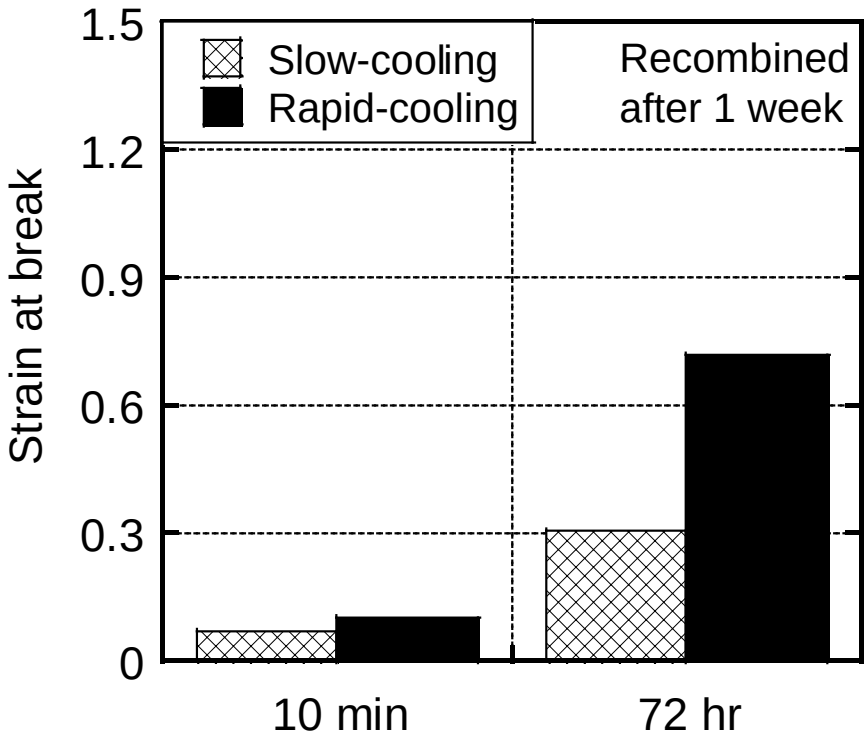

Watanabe et al., Figure 7

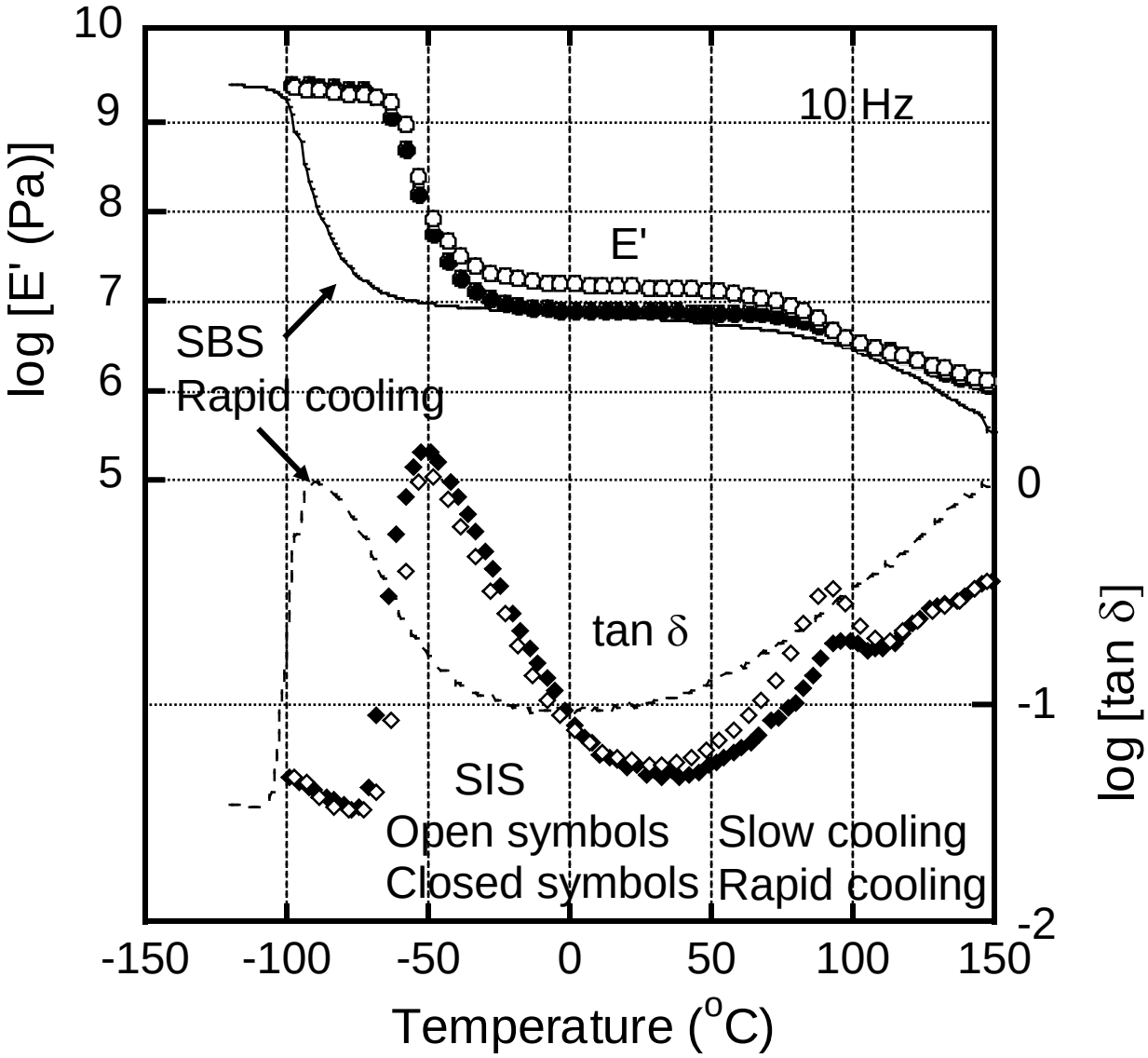

Watanabe et al., Figure 8

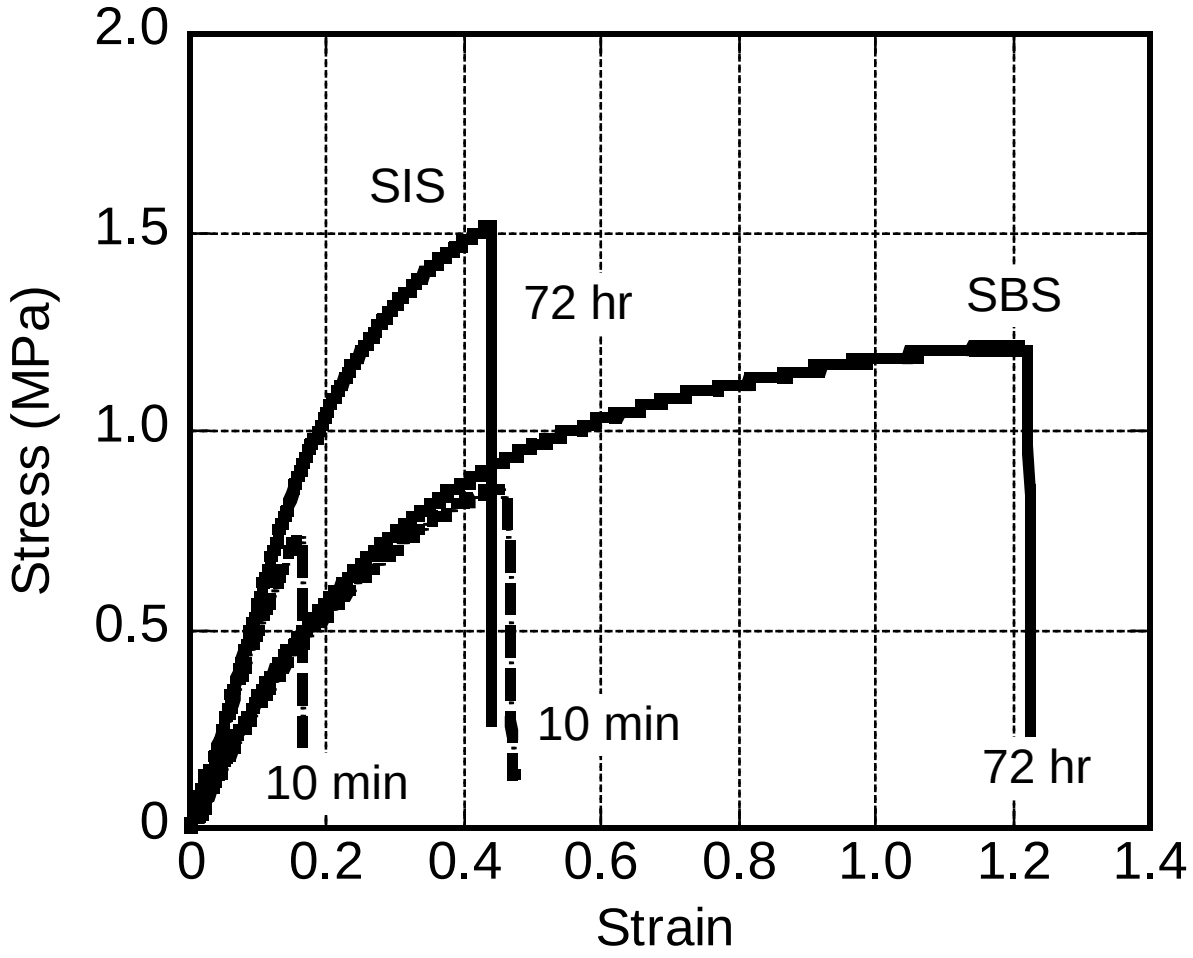

Watanabe et al., Figure 9